Journal of Materials Chemistry B

PAPER

View Article Online
View Journal | View Issue

Cite this: J. Mater. Chem. B, 2015, 3, 387

Development of injectable citrate-based bioadhesive bone implants†

Denghui Xie,‡[abc] Jinshan Guo,‡[c] M. Reza Mehdizadeh,[d] Richard T. Tran,[c] Ruisong Chen,[ab] Dawei Sun,[ab] Guoying Qian,[e] Dadi Jin,*[ab] Xiaochun Bai*[ab] and Jian Yang*[ac]

Received 10th September 2014
Accepted 24th October 2014

DOI: 10.1039/c4tb01498g

www.rsc.org/MaterialsB

Injectable bone implants have been widely used in bone tissue repairs, including the treatment of comminuted bone fractures (CBF). However, most injectable bone implants are not suitable for the treatment of CBF because of their weak tissue adhesion strengths and minimal osteoinduction. Citrate has been recently reported to promote bone formation through enhanced bioceramic integration and osteoinductivity. Herein, a novel injectable citrate-based mussel-inspired bioadhesive hydroxyapatite (iCMBA/HA) bone substitute was developed for CBF treatment. Note that iCMBA/HA can be set within 2–4 minutes and the as-prepared (wet) iCMBA/HA possesses low swelling ratios, compressive mechanical strengths of up to 3.2 ± 0.27 MPa, complete degradation in 30 days, suitable biocompatibility, and osteoinductivity. This is also the first time that citrate supplementation in osteogenic medium and citrate released from iCMBA/HA degradation has been demonstrated to promote the mineralization of osteoblastic differentiated human mesenchymal stem cells (hMSCs). *In vivo* evaluation of iCMBA/HA in a rabbit comminuted radial fracture model showed significantly increased bone formation with markedly enhanced three-point bending strength compared to the negative control. Neovascularization and bone ingrowth, as well as highly organized bone formation, were also observed, showing the potential of iCMBA/HA in treating CBF.

1. Introduction

Comminuted bone fractures (CBF) are recognized as one of the most difficult orthopedic conditions to treat[1,2] because of the difficulty in bone reduction and fixation, which leads to bone segment displacement, deformed bone union, and non-union.[2] To improve reduction and fixation, open surgery with internal instrumentation fixation of large bone pieces has been implemented to provide sufficient stability in relatively simple bone fracture cases. However, for some complicated CBF with numerous bone pieces, open surgery is unable to offer sufficient fixation for these small bone pieces, and consequently fails to reunite them for proper bone alignment and regular bone healing. Therefore, the development of an ideal method to mend the broken bone pieces together, maintain aligned bone reduction, and effectively fill the space between the scattered bone pieces against other connective tissue has become a significant clinical challenge.

To address the aforementioned issues, a variety of bone substitutes have been developed for bone regeneration.[3–20] Among them, injectable bioactive bone substitutes are preferred[6–9] and have been extensively studied.[10–20] However, the application of current injectable bioactive bone substitutes is limited by many shortcomings. For example, non-degradable or slow-degrading bone substitutes, such as commercially available poly(methyl methacrylate) (PMMA) and calcium phosphate cements (CPCs), compromise normal bone healing by inhibiting new bone and vascular ingrowth.[10–12] On the other hand, biodegradable hydrogel-based injectable bone composites, such as chitosan and gelatin-based hydrogels systems,[6–9,19–22] show insufficient adhesive fixation strengths. Commercially available fibrin adhesives have been regarded as the gold standard for soft tissue adhesion, but their adhesion strengths are weak and diminish in wet conditions such as bleeding bone defects. We have recently shown that dopamine, a derivative of L-3,4-dihydroxyphenylalanine (L-DOPA) that contributes to the

[a]Department of Orthopedic Surgery, The Third Affiliated Hospital of Southern Medical University, Academy of Orthopedics, Guangdong Province, China. E-mail: dadijin@yahoo.com

[b]Department of Biology, Southern Medical University, Guangzhou, 510515, China. E-mail: baixc15@smu.edu.cn

[c]Department of Biomedical Engineering, Materials Research Institutes, The Huck Institutes of The Life Sciences, The Pennsylvania State University, University Park 16802, USA. E-mail: jxy30@psu.edu

[d]Department of Bioengineering, The University of Texas at Arlington, Arlington, TX 76010, USA

[e]Department of Biology, College of Biological and Environmental Sciences, Zhejiang Wanli University, Ningbo 315100, China

† Electronic supplementary information (ESI) available. See DOI: 10.1039/c4tb01498g

‡ These authors contribute equally to this work.

strong under-water adhesive properties of marine mussels,[23] can be utilized to synthesize biomimetic injectable citrate-based mussel-inspired tissue bioadhesives (iCMBA), which possess much stronger adhesive strength to soft tissue compared to commercially available fibrin sealant.[22] iCMBA composited with hydroxyapatite (HA) composites is expected to exhibit better adhesive properties to bone pieces, which is favorable to the bone fixation and healing process in CBF.

In addition to offering sufficient structural and mechanical support, an ideal bone substitute should possess osteogenic potential by incorporating osteoinductive elements. Citrate, an intermediate in the Kreb's Cycle, is highly abundant in bone and closely associated with bone metabolism and formation.[24–26] Recent studies have shown that citrate plays an indispensable role in bone formation. Tran *et al.* were the first to experimentally determine that citrate in degradable polymers greatly increased the alkaline phosphatase (ALP) and osterix (OSX) gene expression in C2C12 cells, which is a mouse myoblast cell line that is capable of differentiating into osteoblasts.[27] Hu *et al.* quantified the citrate content in native bone and discussed the indispensable role of citrate in the formation and regulation of the nanocrystalline structure of bone apatite.[28] Costello *et al.* discussed the speculated roles of citrate metabolism and production for the osteogenic differentiation of stem cells and bone formation.[29,30] These latest findings are strong evidences that citrate could be involved in bone substitute design and has led to the development of a series of citrate-based composites for bone applications, including poly(diol citrates)-HA (POC-HA), poly(ethylene glycol) maleate citrate-HA (PEGMC-HA), and citrate-based polymer blends-HA (CBPB-HA).[31–36]

In the current study, iCMBA was composited with HA and used as an injectable bone substitute (Fig. 1). It is believed to have superior properties for CBF treatment because of the following properties afforded by a citrate and dopamine-containing composite: (1) excellent adhesion strength in wet conditions; (2) controlled degradability; (3) enhanced osteoinductive potential by the released citrate;[27] (4) calcium chelating ability of citrate; (5) minimal inflammatory response;[22] (6) instant hemostatic properties in the surrounding tissue;[22] and (7) osteoconductive and osteointegration potential. The physical and mechanical properties, biocompatibility, and osteogenic potential of iCMBA/HA composites were studied and evaluated for CBF treatment in a rabbit model. Furthermore, citrate was exclusively investigated *in vitro* to explore its effect on the mineralization of osteoblastic differentiated human mesenchymal stem cells (hMSC).

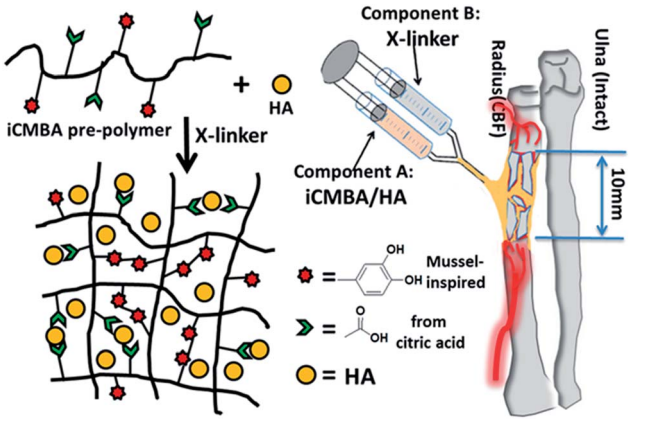

Fig. 1 Schematic representation for iCMBA/HA crosslinking process and iCMBA/HA injection procedure for the treatment of comminuted bone fracture.

2. Experimental section

2.1 Materials

All chemicals, cell culture medium, and supplements were purchased from Sigma-Aldrich (St. Louis, MO), and they were used as received, except where mentioned otherwise.

2.2 iCMBA/HA composites synthesis

Injectable iCMBA/HA composites were fabricated with iCMBA and HA powder (Fig. 1). Firstly, iCMBA pre-polymer was synthesized by the polycondensation of citric acid (CA), poly(-ethylene glycol) (PEG) and dopamine according to our previous work.[22] Briefly, CA and PEG were placed in a three-necked round-bottom flask and heated to 160 °C under stirring till melting was observed. Then, under nitrogen gas flow, a calculated amount of dopamine was added to the mixture. The temperature was reduced to 140 °C and the reaction was continued under vacuum until the stir bar stopped turning at 60 rpm. Secondly, iCMBA-$P_{200}D_{0.3}$ (using PEG 200 and 0.3 eq. [to CA] of dopamine) was chosen to make iCMBA/HA composites. For this purpose, iCMBA-$P_{200}D_{0.3}$ was dissolved in deionized (DI) water (40 wt%), and then different amounts of HA were mixed with it to achieve various final composite formulations with 30, 50, and 70 wt% HA. Finally, crosslinker solution (4 wt% or 8 wt% $NaIO_4$ in DI water) was added to the mixture at a 1 : 1 volume/mass ratio of PI solution and polymer to crosslink the composites.

2.3 Setting time

To control the crosslinking process, various calculated amounts of crosslinker solution (PI, in DI water) were added to the mixture. The amount of PI was determined to provide sufficient time for this composite preparation and injection without compromising its final mechanical properties. The setting time of the composites was determined as the time from the addition of PI to the iCMBA–HA mixture until it was not flowable.

2.4 Physical and mechanical properties of iCMBA/HA composites

The sol/gel content, an indication of non-crosslinked/crosslinked fractions of the composites, and swelling ratio was measured by the difference in mass before and after incubation of the polymer network in a solvent as described in a previous study.[22] The sol content (Table 1) and swelling ratio were then calculated using eqn (1) and (2), respectively. Here W_i represents

Table 1 Set time of iCMBA/HA composites with various formulation

Composite formulation	HA/composite ratio (dry w/w%)	PI to pre/polymer ratio (w/w%)	Measured set time (s)
iCMBA-P_{200} $D_{0.3}$ HA30%	30	4%	247 ± 13
iCMBA-P_{200} $D_{0.3}$ HA30%	30	8%	172 ± 15
iCMBA-P_{200} $D_{0.3}$ HA50%	50	4%	238 ± 9
iCMBA-P_{200} $D_{0.3}$ HA50%	50	8%	166 ± 11
iCMBA-P_{200} $D_{0.3}$ HA70%	70	4%	231 ± 10
iCMBA-P_{200} $D_{0.3}$ HA70%	70	8%	159 ± 8

the initial dry weight of cross-linked hydrogel disk, W_d represents the weight of freeze-dried sample after the uncross-linked part being washed by 1,4-dioxane for 48 h, whereas W_s represents the network weight after leached and dried sample are suspended in water for 24 h. Degradation studies were conducted in PBS (pH 7.4) and at 37 °C using cylindrical disc specimens (7 mm in diameter, 2 mm thick) as described in a previous study.[22] The mass loss was calculated by comparing the initial mass (W_0) with the mass measured at the pre-determined time points (W_t) using eqn (3).

$$\text{Sol}\ (\%) = \frac{W_i - W_d}{W_i} \times 100 \quad (1)$$

$$\text{Swelling}\ (\%) = \frac{W_s - W_d}{W_s} \times 100 \quad (2)$$

$$\text{Mass loss}\ (\%) = \frac{W_0 - W_t}{W_0} \times 100 \quad (3)$$

The mechanical properties of iCMBA/HA composites were investigated by unconfined compressive testing. The measurements were conducted according to ASTM D695-10 on a MTS Insight 2 fitted with a 500 and 10 kN load cell (Instron, Norwood, MA). Briefly, the cylindrical shaped samples (6 mm × 12 mm, diameter × height) were compressed at a rate of 1.3 mm min^{-1} and deformed to failure. Values were converted to stress–strain and the initial modulus was calculated from the initial slope of the curve (0–10% elongation except the modulus of the freeze-dried and air-dried samples of iCMBA-$P_{200}D_{0.3}$ PI8% HA70% [0–1%]). The mechanical tests were conducted on as-prepared samples (samples were sealed in vials for 2 h, 24 h and 48 h after preparation) as well as on samples completely dried naturally (air-dried for 3 days) or by lyophilization (freeze-dried). The structural difference between freeze-dried and air-dried samples was observed under scanning electron microscopy (SEM).

To test the adhesion strength of iCMBA/HA composites to the bone surface of a chicken bone, a bone cut model was created by obliquely cutting a chicken bone into two parts and then reuniting it with iCMBA (iC) and iCMBA/HA 70% (iCH70) using 8 wt% of PI solution as a cross-linker. After 2 hours (wet condition, sealed with parafilm to keep wet) and 48 hours (dry condition), the load and shear strength of repaired chicken bones were tested on an MTS system.

2.5 Mineralization of iCMBA/HA composites

To evaluate the *in vitro* mineralization of iCMBA/HA composites, disk shaped scaffolds of the composites (iCMBA-$P_{200}D_{0.3}$ PI8% HA70%, iCH70) were immersed in simulated body fluid (SBF), which was prepared as described in the literature.[37] To accelerate the mineralization process, concentrated SBF was used, in which the concentration of inorganic ions was five times of that in human blood plasma (SBF-5X). The composite samples were immersed in 10 mL of SBF-5X and incubated at 37 °C for up to 5 days while the SBF was replaced every other day. At each predetermined time interval, the specimens ($n = 5$) were taken out, washed gently with DI water to remove any soluble inorganic ions from the surface of samples, and air-dried. Next, the specimens were sputter-coated with silver and examined by scanning electron microscopy (SEM) using Hitachi 3000N (Hitachi, Pleasanton, CA). The elemental analysis of the mineralized composites was also conducted by Energy dispersive X-ray spectroscopy (EDX) to determine the composition and ratio of the elements present in the minerals formed on the surface of the composites. In addition to composites, iCMBA-$P_{200}D_{0.3}$ PI 8% without HA (iC) was also subjected to mineralization test to determine the possible role of HA in the mineralization of iCMBA/HA composites.

2.6 *In vitro* cell study

2.6.1 Cytotoxicity of sol content and degradation products. The cytotoxicity of sol content or leachable fraction and degradation products of iCMBA pre-polymer and iCMBA/HA composites were studied using MTT (methylthiazolyldiphenyl-tetrazolium bromide) assay against human mesenchymal stem cells (hMSCs, Lonza Walkersville Inc, US).

The sol content or leachable fraction of iCMBA and iCMBA/HA composites were obtained by incubating equal mass (0.5 g) composites specimen in 5 mL PBS (pH 7.4) for 24 hours. Next, three different solutions were prepared: 1×, 10× and 100× (1× was the solution of leached products with no dilution; 10× and 100× means 10 times and 100 times dilution of 1× by PBS, respectively). To each well of a 96-well cell culture plate, a 200 μL of solution of hMSC cells with a density of 5×10^4 cells per mL in complete Dulbecco's modified Eagle's medium (DMEM with 10% fetal bovine serum (FBS) and 1% antibiotic antimycotic solution (100X)) was added and incubated for 24 hours at 37 °C, 5% CO_2. Next, 20 μL of sol content fraction with various concentrations of iCMBA and iCMBA/HA composites were

added and incubated for another 24 h, followed by MTT assay analysis as per the manufacturer's protocol.

The cytotoxicity of degradation products was also evaluated. Equal weight (1 g) of iCMBA and iCMBA/HA composite samples, as well as poly(lactic-*co*-glycolic acid) (PLGA, used as control, LA/GA = 50/50, $M_w \sim 60$ kDa, purchased from Polyscitech), were fully degraded in 10 mL of 0.2 M NaOH solution, and the resultant solutions were diluted to three concentrations (1×, 10× and 100×) using PBS (pH 7.4), and used for cytotoxicity study as described above) and subsequent MTT analysis.

All the above solutions were pH-neutralized and passed through a 0.2 μm filter prior to use for cell culture. The cell viability results were normalized to the viability of cells in complete DMEM medium.

2.6.2 Effect of iCMBA/HA degradation products on hMSCs' osteogenic differentiation process. The effect of degradation products of iCMBA and iCMBA/HA composites on the proliferation (cell viability) and differentiation (ALP activity and calcium deposit formation) of hMSC during osteogenic differentiation process were studied with Live/Dead staining, ALP activity test, and Alizarin Red staining.

Briefly, iCMBA (iC) and iCMBA/HA70% (iCH70) composites were directly degraded in osteogenic (OG) media at 37 °C with 5% CO_2 to separately produce OiC and OiCH70 media. To eliminate the effect of HA particles in media on cell differentiation, OiCH media was created by filtering OiCH70 media with 0.22 μm filters. Osteogenic media were composed of complete DMEM supplemented with 10^{-7} M dexamethasone, 10^{-2} M β-glycerophosphate, and 50 μM L-ascorbic acid. Then, hMSCs were cultured in the abovementioned media for 14 days using growth media (MG) as a negative control. Note that culture media were replaced every other day. Live/Dead staining (Life Technologies Inc., US) and scanning electron microscopy (SEM) scanning was conducted to assess the cell viability and morphology of differentiated hMSCs. Moreover, to test the effect of iCMBA/HA degradation products on osteoinduction and osteogenesis (ALP activity and calcium deposit formation), ALP activity test and Alizarin Red staining were conducted following standard protocols at three pre-determined time points (4, 7 and 14 days).

The adhesion, proliferation, and differentiation of a pre-osteoblast cell line, MC3T3 (ATCC), which was cultured on the composites, were also studied. The details of experimental methods and results can be found in the ESI.†

2.6.3 Citrate release from iCMBA/HA composite. iCH70 was chosen as the representative for citrate release studies. Briefly, 0.1 g dried iCH70 composite was immersed into 10 mL PBS (pH 7.4) at 37 °C, and at each pre-determined time interval (2, 5, 7, 14, 21, 24, 28, and 30 days), 0.2 mL of PBS solution was removed and filtered (using 0.2 μm filters) to prepare samples for high-performance liquid chromatography (HPLC). 0.2 mL fresh PBS was replaced in the tube to maintain the volume constant at 10 mL. The determination of cumulative citrate release was carried out using a Shimadzu HPLC system equipped with a UV-visible PDA detector and a Phenomenex Kinetex C18 column at 40 °C. PBS with a pH value of 2.8 was used as the mobile phase with a flow rate of 1 mL min^{-1}. The detection of citrate was set at 210 nm, and a calibration curve of citrate was obtained under the same conditions.

2.6.4 Effect of citrate on calcium deposit formation. To test the effect of citrate on calcium deposit formation of osteogenic-differentiated and undifferentiated hMSC, Alizarin Red staining was conducted following a well-established protocol. For proliferation, hMSCs were cultured in growth media (MG, completed DMEM), whereas for osteogenic differentiation, hMSCs were cultured in osteogenic media (OG). A calculated volume of citrate was added into MG and OG separately to achieve a final citrate concentration of 20 μM in both media. hMSCs were cultured in these media separately and incubated at 37 °C with 5% CO_2, and the media were replaced every other day. At 7, 14, and 21 days, the cells were stained with 2% Alizarin Red Staining solution (adjusted to pH 4.0) to determine calcium deposit formation.

2.7 *In vivo* study

Because of its strong mechanical properties and biocompatibility *in vitro*, iCMBA-$P_{200}D_{0.3}$ PI 8% HA 70% (iCH70) composite was chosen for *in vivo* study.

2.7.1 Comminuted radial fracture model and iCH70 injection. All animal experiments were carried out in compliance with a protocol approved by Southern Medical University's Animal Care and Use Committee (Guangzhou, China). Thirty-six New Zealand Rabbits (male, 3 kilogram on average) were randomly assigned into two groups: blank control group and iCH70 group. All rabbits were anesthetized with 3% sodium pentobarbital (1.5 mL kg^{-1}) as per a previous protocol.[27] After shaving and disinfecting the surgical area, 20 mm skin incisions were made at the sites 15 mm below the radius head of both forelimbs. Through the intermuscular space, the radius was exposed clearly with minimal tissue injury. To make a standard and reproducible comminuted radial fracture, osteotomy was performed at two sites with a surgical electric saw to produce a 10 mm length bone block. The bone blocks were cut into several segments (usually 3–4 fragments) with a bone rongeur. It should be noted that the ulna was kept intact to provide sufficient biomechanical support for a fractured radius (Fig. 1). Segmented bone pieces were re-aligned and fixed after iCH70 injection. The deep fascia and skin were sutured tightly and then analgesic and anti-bacterial ointments were given. For control, the same procedure was repeated and bone pieces were re-aligned but without the use of filling materials. After rabbits were sacrificed with CO_2 at pre-determined time intervals (4, 8, 12 weeks post-operation), their radial bone specimens were removed and prepared for the following assessments.

2.7.2 Computer tomography analysis for explants. Computer tomography (CT) analysis was conducted using a Micro-CT imaging system (ZKKS-MCT-Sharp-III scanner, Caskaisheng, CHINA) following standard and validated precise protocols.[27] Briefly, the scanning system was set to 70 kV, 30 W, and 429 μA. A quantitative 3D histomorphometric evaluation (*i.e.*, determination of bone mineral density and bone mineral content) was then performed on a rectangular volume of interest (VOI) using well-recognized methods.[38] Bone mineral

content (BMC) and bone mineral density (BMD) were measured and the data were processed and analyzed using NIH-Image software (National Institute of Health, Bethesda, MD, USA).

2.7.3 Biomechanical test for explants. At pre-determined time intervals (4, 8, 12 weeks post-operation), rabbits were sacrificed and radius specimens were removed for three-point bending testing at the radial diaphysis following a previously described protocol.[39–42] Briefly, the two ends of radius were horizontally fixed on the Material Testing System platform (with a span of 2.5 cm between the supports) and a constant vertical compression load (5 mm min^{-1}) was applied to the midpoint of the fractured bone until a fracture occurred. The load and displacement data were recorded at 100 Hz. The maximum flexural strengths were calculated and compared between iCH70 group and blank control group.

2.7.4 Histological examination. For undecalcified sections, histological examination was performed at pre-determined time intervals (4, 8, 12 week post-operation) according to a previous protocol.[41] After fixation and dehydration by ethanol, the radius specimens were embedded in methyl methacrylate without decalcification. Next, 10 μm longitudinal sections were cut at the diaphysis of interest using a SP2500 microtome (Leica Microsystems, Wetzlar, Germany). The sections were then stained by Masson's trichrome method. For decalcified sections, histological examination was performed at the 4-week time interval for vascularization with hematoxylin and eosin (H&E) staining. Bone histomorphometric analysis was performed under a semi-automated digitizing image analyzer system for both types of sections. This system consisted of an Olympus BX51 microscope (Center Valley, PA, USA), a computer-coupled QImaging Retiga EXi camera (Surrey, Canada), and BioQuant Osteo 2009 software (Nashville, TN, USA).

2.8 Statistical analysis

All experiments were performed in duplicates. The statistical results were based on the three experiments. All data are expressed as mean ± standard deviation. The statistical significance between two sets of data was calculated using a Student's *t*-test. Data were taken to be significant if $p < 0.05$ was obtained.

3. Results and discussion

With the rapid advancement of orthopedic internal/external fixation instruments, the fixation of large bone segments in relatively simple fractures has shown great success. However, CBF remains an unresolved issue in achieving effective fixation of small and scattered bone pieces and maintaining bone alignment after complete bone reduction.[1,13,14] Adhesive biomaterials are considered a potential solution by offering the ability to stabilize small fractured bone pieces. Inspired by the adhesive strength of marine mussels and based on recent understanding of citrate's role in bone formation, our group has developed a citrate-based iCMBA polymer, which shows strong adhesive properties in wet conditions.[22] For orthopedic applications, an adhesive iCMBA/HA bone composite was synthesized by combining iCMBA with osteoconductive HA particles and its performance with regards to intra-operational manipulation, mechanical strength, and bone formation was also investigated.

3.1 Rationale behind iCMBA/HA bone composites

Citrate has been well known as an essential intermediate of the Kreb's Cycle in cellular metabolism. However, the role of citrate in bone formation and mineralization has not been given enough attention, although a few reports did find its close association with bone based on the evidence that citrate makes up about 5 wt% of the organic component in bone and over 90% of the body's total citrate content is located in the skeletal system.[24–26] Until recently, a few important studies have renewed the interest for the role of citrate in bone development.[27,28] Hu *et al.* confirmed that citrate has an indispensable effect in the nanocrystalline structure of bone apatite as well as bone strength.[28] Tran *et al.* identified citrate to enhance bone-related gene expression such as alkaline phosphatase (ALP) and osterix (OSX) by C2C12 cells.[27] It is envisioned that citrate enhances osteoinduction and bone formation and should be included in bone substitute design.

Inspired by the adhesive strength of marine mussels, adhesive iCMBA was developed in our group by a one-pot polymerization of citrate, poly(ethylene glycol) (PEG), and dopamine. After oxidation, dopamine showed stronger adhesion to biological surfaces such as skin or sheathes, which connect with bone through the formation of covalent bonds with available nucleophile groups, such as $-NH_2$, –SH, –OH and –COOH, on these surfaces. Dopamine can also directly interact with inorganic bone surface to provide adhesion strength. Although the iCMBA pre-polymer was initially applied for wound closure, its strong adhesion strength in wet tissue and fast degradation rate motivated us to apply it to bone substitute fabrication. In wound closure studies, iCMBA offers much stronger adhesion strength, especially in wet conditions when compared to fibrin sealants, which are regarded as a gold standard for wound closure. Even more importantly, the fast degradability of ester bonds in the iCMBA backbone can potentially allow osteoblast migration and neovascularization in the bone scaffold in the early stages of bone healing. Based on the abovementioned promising potential, we have developed the iCMBA/HA bone substitute and applied it for CBF treatment in a rabbit model.

3.2 Physical, mechanical property, mineralization and cytotoxicity of iCMBA/HA

3.2.1 Setting time. In order to be suitable and practical for CBF applications, ease of handling and administration are important design requirements. To obtain a material that can be easily handled, an ideal setting (crosslinking) time is important because the expected bone substitutes should provide sufficient handling time during the transformation from a flowable liquid to a set material. It was reported that for self-setting bone cements, at least 1 minute should be allowed for clinicians to collect the paste and place it on a pallet knife or into syringes.[12] Thus, the setting time should be long enough

(at least 2–3 min) to allow surgeons to collect and deliver the materials to bone defects before setting. iCMBA/HA composites were tested to be injectable using a cannula injection tool, which was used for femoral head injection in our previous study.[34] The setting time of our iCMBA/HA bone substitute is completely adjustable and can be easily tuned by regulating multiple factors (Table 1). iCMBA/HA composites were all prepared using iCMBA-$P_{200}D_{0.3}$ and varying amounts of HA and sodium periodate (PI). The setting time was varied between 159 ± 8 seconds for iCMBA-$P_{200}D_{0.3}$ PI8% HA70% (iCH70) and 247 ± 13 seconds for iCMBA-$P_{200}D_{0.3}$ PI 4% HA30% with PI-to-prepolymer ratios of 8% and 4%, respectively. Increasing the amount of HA in the composition slightly decreased the setting time, whereas an increase in PI concentrations accelerated the crosslinking reaction to shorten the setting time.

3.2.2 Sol/gel content, swelling ratios, and degradation properties. An ideal synthetic bone substitute should also possess acceptable sol/gel content, swelling ratio, and adequate degradation rates for new bone ingrowth and vascularization.[17] The sol contents of different iCMBA/HA composites were all at low percentages, ranging from 2.46% ± 0.82% to 3.29% ± 0.91% with no significant difference ($p > 0.05$) between the samples with and without HA (Fig. 2A). Composite swelling data revealed that the degree of swelling was lowest for iCH70, followed by iCMBA/HA 50% (iCH50), iCMBA/HA 30% (iCH30) and pure iCMBA prepolymer (iC, no HA) with swelling ratios of 110% ± 6%, 249% ± 31%, 353% ± 35%, and 802% ± 69%, respectively (Fig. 2B). The results from composite degradation show that the degradation rate decreased as the amount of HA increased in the composites. As shown in Fig. 2C, iCH70 exhibited the slowest degradation rate with complete degradation after 30 days of incubation in PBS at 37 °C followed by iCH50 and iCH30. iC with no HA degraded much faster than composites with HA (Fig. 2C). The sol content of iCMBA/HA composites reached the expected crosslinking level (up to 97.54%), while swelling data showed that iCMBA/HA composites, especially iCH70, could maintain its structure with minimal swelling ratios. This indicates that iCMBA/HA composites can meet the requirements for an injectable bone substitute. More importantly, degradation studies show that iCH70 possesses an ideal degradation rate with a weight loss more than 25% after one week and almost 100% after one month (Fig. 2C). It is already well known that relatively faster degradation rates can induce vascular ingrowth, which is significantly vital to cell migration, survival, and tissue formation.[17,43] Relatively fast degradation rates may produce adequate space for vascularization and cell migration within the initial weeks after implantation, which is vital for capillary networks induced by the inflammatory processes and neovascularization of the scaffold.[44–46] Therefore, it is natural to believe that our iCMBA/HA bone substitute may allow for and promote neovascularization and cell migration into the composite through the space left after degradation (Fig. 2C).

3.2.3 Mechanical properties. The mechanical properties of iCMBA/HA composites for as-prepared (2, 24 and 48 h after preparation) and air- or freeze-dried samples are shown in Fig. 3. It can be seen that the compressive strength and modulus for iCMBA/HA was much higher than that of pure iCMBA ($p < 0.01$), and increasing the amount of HA in the composition resulted in higher compressive strength and modulus. No differences in the compressive strength and modulus values of iCH30 and iCH50 as-prepared samples were observed ($p > 0.05$) with compressive strengths around 1 MPa and modulus lower than 0.5 MPa. The compressive strength of both iCH30 and iCH50 showed nearly no distinct change when the curing time increased from 2 to 24 h ($p > 0.05$), whereas the modulus showed a slight increase with curing time (Fig. 3A and B). When the HA content in iCMBA/HA composites reached 70% of dry weight, the compressive strength of iCH70 reached 1.6 ± 0.21 MPa after preparation for 2 h, and this value increased to 2.6 ± 0.29 and 3.2 ± 0.28 MPa after 24 and 48 h, respectively, which was much higher than that of iCH30 and iCH50 ($p < 0.01$, Fig. 3A). The modulus of iCH70 also increased from 0.75 ± 0.11 MPa for 2 h to 2 ± 0.31 MPa for 24 h, and the values were maintained for up to 48 h after preparation. The compressive strain at failure (Fig. 3C) of iCMBA/HA composites with different HA ratios is higher than that of pure iCMBA. The strain at failure of iCH30 and iCH50 was higher than 60% for 2 h samples, and decreased in response to an increase in time. The strain of iCH70 was higher than 50%, which indicates the soft nature of as-prepared iCMBA/HA composites. The stress–strain curves of the as-prepared composites 48 h after preparation are shown in Fig. 3D. After freeze-/air-drying, the compressive strength and modulus (Fig. 3E and F) for iCMBA/HA composites became much higher than that of the corresponding as-prepared samples. An increase in HA content

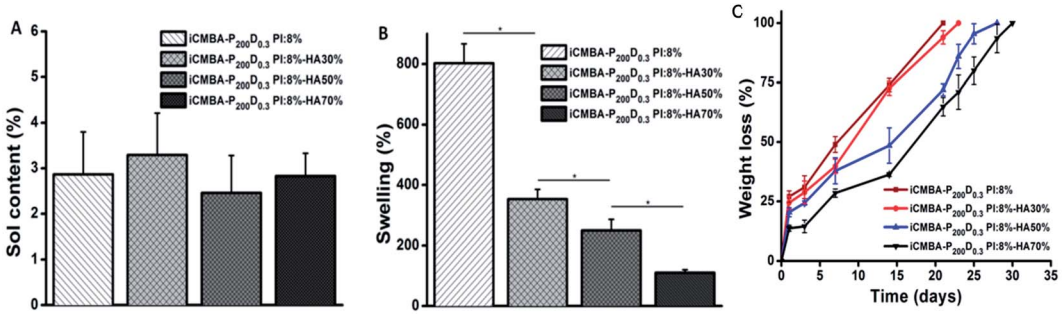

Fig. 2 Soluble content (A), swelling ratio (B) and degradation profiles (C) of iCMBA/HA composites. *: $p < 0.05$.

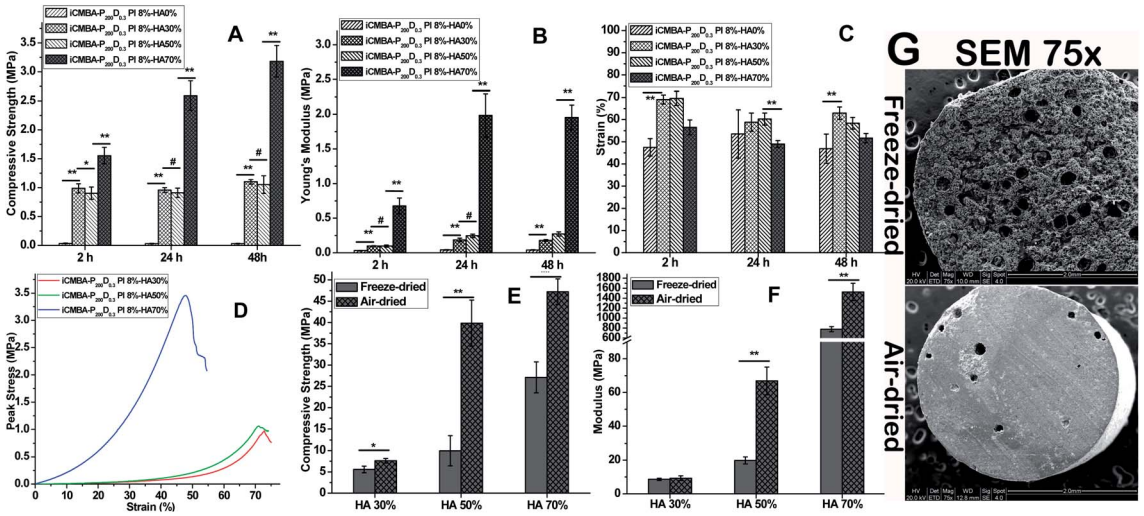

Fig. 3 Mechanical properties and SEM images of iCMBA/HA composites. Compressive strength (A), modulus (B), and strain at failure (C) of as-prepared samples after 2, 24 and 48 h; stress–strain curves (D) of iCMBA/HA composites measured through compressive mechanical testing of as-prepared samples 48 h after preparation. Compressive strength (E) and modulus (F) of freeze-dried and air-dried samples. #$p > 0.05$, *$p < 0.05$, **$p < 0.01$. (G) SEM images of freeze-dried and air-dried iCMBA-P_{200} $D_{0.3}$-HA70% (iCH70) composites.

resulted in higher mechanical strength. The compressive strength and modulus of freeze-dried/air-dried iCH70 reached 27.1 ± 3.6/47.2 ± 3.1 and 778.2 ± 51.5/1525.6 ± 172.9 MPa, respectively. Pores formed during the freeze-drying process, which was confirmed by SEM images of freeze-/air-dried iCH70 samples (Fig. 3G), contributed to the lower mechanical strength of freeze-dried composites compared to the corresponding air-dried composites.

The adhesion property of bone cements to bone surfaces is also critical for bone regeneration, especially for CBF in which fractured bone pieces should be glued by the adhesive materials. However, traditional bone cements such as PMMA have very weak bonding to bone because of the incompatible wetting properties between hydrophobic PMMA and hydrophilic bone. Thus, amphiphilic bone bonding glue was used to improve the bonding between PMMA cements and bone.[47] Our iCMBA/HA composites by themselves offer substantial adhesive strength to bone, thus eliminating the potential use of additional glue for bone bonding. To evaluate the adhesive strength of iC and iCH70 to the biological bone surface, both the tensile loads and shear strengths of iCH70 to the chicken bones were tested and compared (Fig. 4). From Fig. 4A, it can be seen that the tensile loads of repaired chicken bones with iCH70 were around 352 g in wet condition (2 hour after application) and 1280 g in dry condition (48 hour after application), respectively. In wet condition, the shear strengths of chicken bones repaired by iCH70 and iC showed no significant difference ($p > 0.05$), with shear strengths about 111 ± 32.4 kPa and 110 ± 17 kPa, respectively (Fig. 4B). Although in dry condition (48 hours after application), the shear strengths of chicken bones repaired by iC (746 ± 197 kPa) seems a little bit bigger than that repaired by iCH70 (680 ± 68 kPa), there is also no significant difference between the two groups ($p > 0.05$) (Fig. 4B). The mechanical studies show that iCH70 can offer sufficient cohesive and adhesive mechanical support for CBF at early bone healing stages, since internal or external fixation with instruments can provide major mechanical support for CBF.

3.2.4 Mineralization of iCMBA/HA composites. In order to investigate whether iCMBA/HA composites support biomineralization, the *in vitro* mineralization of iCMBA/HA composites in SBF-5X was conducted. After 1 day of incubation, no crystals on the surface of iCH70 samples were observed (Fig. 5A). As incubation time continued, crystals of calcium phosphate began to form and grow on the surface of iCMBA/HA composites (Fig. 5B–D). EDX analysis confirmed the existence of these crystals, in which the ratio of Ca/P was around 1.61 (Fig. 5E), which is in the range of the Ca/P ratio to HA (1.33–1.67). Interestingly, no crystal formation on the surfaces of pure iCMBA without HA was found during incubation in SBF-5X (Fig. 5F), which indicates that the inclusion of HA can promote the biomineralization process and in turn promote bone formation.

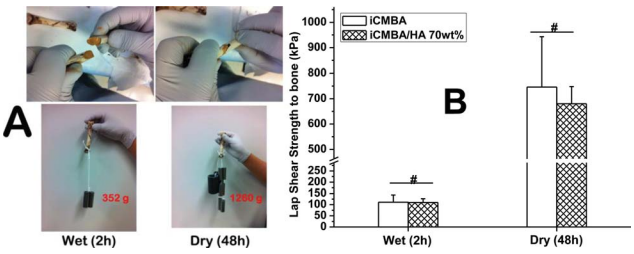

Fig. 4 (A) Application of iCMBA/HA 70 wt% (8 wt% PI) to beveled (beveling angle: 30°) chicken bone (top) and the strong adhesion demonstrated by hanging metal pieces (low); (B) wet (2 h) and dry (48 h) adhesion strengths of iCMBA (iCMBA-P_{200} $D_{0.3}$, 40 wt% in DI water) and iCMBA/HA 70 wt% to chicken bones after applying equal volume of 8 wt% PI [Sodium (meta) periodate, $NaIO_4$] solution. # represents $p > 0.05$.

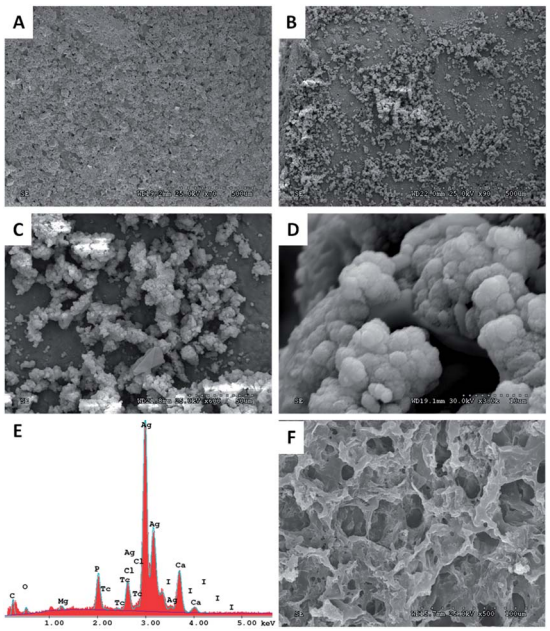

Fig. 5 Mineralization of the iCMBA/HA composites. SEM images of iCMBA-$P_{200}D_{0.3}$ PI 8%/HA70% composites incubated in SBF-5X at 37 °C for (A) 1 day and (B, C, and D) 5 days. (E) EDX analysis of the surface of crystal-deposited composite. (F) iCMBA-$P_{200}D_{0.3}$ PI 8% without HA, incubated in SBF-5X for 5 days at 37 °C (no crystals are present).

3.2.5 Cytotoxicity of iCMBA/HA composites. The cytotoxicity of iCMBA/HA composites was estimated by conducting cytotoxicity studies of the soluble (leachable) content and degradation products of various iCMBA/HA composites using MTT (methylthiazolyldiphenyl-tetrazolium bromide) assay against human mesenchymal stem cells (hMSCs) (Fig. 6). The hMSC viability in the presence of soluble content of the composites (Fig. 6A) at 1× concentration was between 72.51% ± 2.90% (no HA) and 84.44% ± 6.60% (50% HA), showing only minor cytotoxicity. The cell viability became much higher in diluted sol content solutions of 10× and 100×, and the cell viabilities of 100× were all higher than 90%. Furthermore, the degradation products (1×) showed a cell viability of at least 70.84% ± 5.16% (no HA), which is comparable to that of widely used biodegradable polymer PLGA (67.35% ± 5.99%), suggesting that the degradation products of all iCMBA composites did not induce significant cytotoxicity (Fig. 6B). The cell viability improved as the solution of degradation products was further diluted to 10× and 100×. In a separate study, we have also shown that iCH70 also supported the MC3T3 cell adhesion (Fig. S1†) and proliferation (Fig. S2A†). Based on the above results, iCH70 is considered as a promising iCMBA/HA formulation due to improve physical (setting time, sol content, swelling and degradation rate) and mechanical properties with satisfying *in vitro* cytotoxicity.

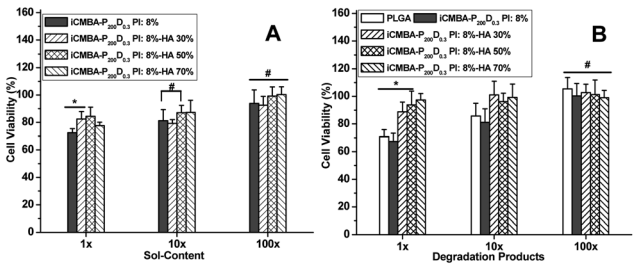

Fig. 6 *In vitro* cytotoxicity of iCMBA/HA composites. Cytotoxicity study using hMSC cells by MTT assay for (A) sol content (leachable products), and (B) degradation products of iCMBA and iCMBA/HA composites. All data were normalized to cell viability in blank medium. #$p > 0.05$, *$p < 0.05$.

3.3 Proliferation and differentiation of hMSCs in the presence of iCMBA/HA, effect of citrate, and HA

3.3.1 Proliferation and differentiation of hMSCs in the presence of iCMBA/HA. To investigate and mimic the effect of HA and citrate (from iCMBA) on the proliferation and differentiation of hMSC during the release process of iCMBA/HA in practical situations when being applied *in vivo*, iCMBA/HA composites (using iCH70) and iCMBA (iC) were completely degraded in osteogenic media (OG) to produce OiC and OiCH70 media, respectively. In order to further study the effects of HA, OiCH media was also created by filtering OiCH70 media with 0.22 μm filters. The proliferation and differentiation of hMSC in OiC, OiCH, and OiCH70 media was conducted and studied by Live/Dead assay, alkaline phosphatase (ALP) activity, and Alizarin Red staining using growth media (MG) and osteogenic media (OG) as controls (Fig. 7). From the Live/Dead images (Fig. 7A), it can be seen that hMSCs grew well for all the five groups. After 14 days, the morphology of hMSCs maintained an elongated shape, while the morphology of hMSCs changed after being cultured in OG, OiC, OiCH and OiCH70 media for 4 days. The cell densities of hMSCs cultured in OG, OiC, OiCH and OiCH70 media were all lower than that of hMSCs cultured in MG media. From one aspect, these results indicate that hMSCs differentiated in OG and osteogenic media containing iCMBA and iCMBA/HA degradation products.

The results of calcium deposit formation in cell culture are shown in Fig. 7B. In osteogenic media (OG), calcium deposits in hMSC cultures could be observed after 10 days, and the amount of calcium deposits increased over time in every group.

However, no calcium deposits were found in MG group at all time intervals. Increased calcium deposits were observed in OiC, OiCH and OiCH70 groups when compared to OG group, especially in OiCH70 group, indicating that the inclusion of iCMBA and HA can promote calcium deposits formation by osteogenic differentiated hMSCs. The results of ALP activity are shown in Fig. 8. When hMSCs were induced into osteoblastic linage in osteogenic media, the ALP expression in each group increased over time. At 4, 7 and 10 days, no significant difference can be observed between the tested groups. However, after 14 days, the ALP expression of OiC, OiCH and OiCH70 groups increased and were all significantly higher than that of OG group in the corresponding time point ($P < 0.05$), further indicating the positive effect of iCMBA and HA in hMSCs osteogenic differentiation. As shown in Fig. S2B,† iCH70 also supports the

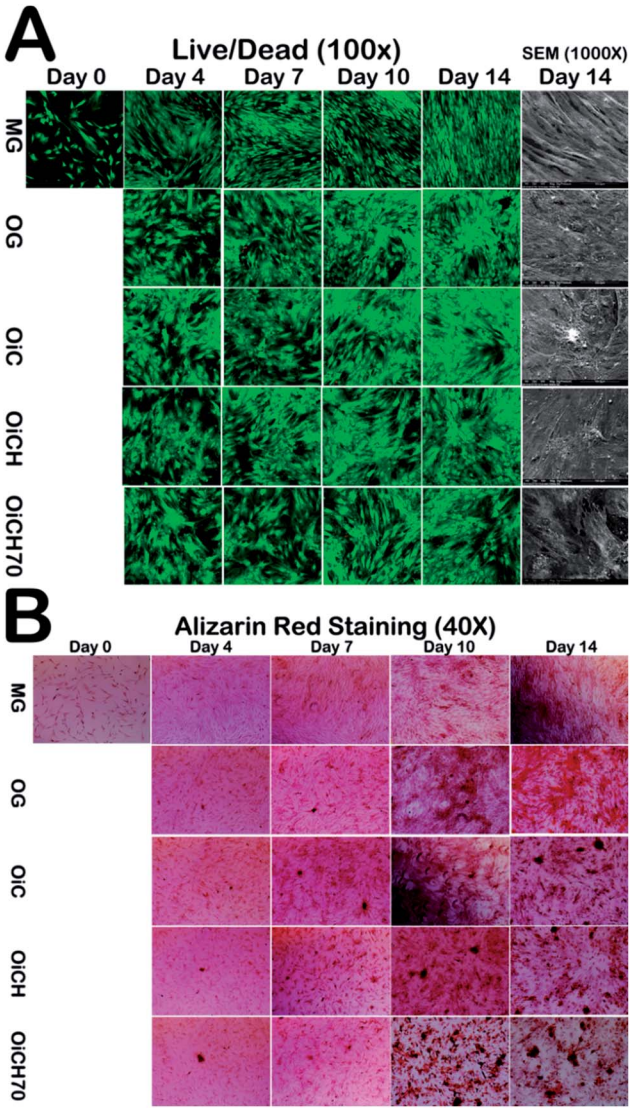

Fig. 7 Live/Dead and SEM images (A) and Alizarin Red Staining (B) of hMSC treated with growth media (MG), osteogenic media (OG), osteogenic media with degradation products from iCMBA (OiC), iCH7 with HA filtered (OiCH) and iCH7 with HA in the media (OiCH70).

osteogenic differentiation of MC3T3 cultured on the composite surfaces, which can be verified by the increased ALP activities at 7 days.

To further investigate the effect of citrate on calcium deposit formation of osteogenic-differentiated and undifferentiated stem cells, hMSCs were cultured in growth media (MG) and osteogenic media (OG) supplemented with citrate at a concentration of 200 μM with pure MG and OG media used as controls. After 7, 14 and 21 days, Alizarin Red staining was conducted to visualize calcium deposits (Fig. 9). When hMSC were cultured in growth media, no matter with or without 200 μM citrate supplementation, no calcium deposits were found at all time intervals. However, when hMSC were induced into osteocyte lineage in osteogenic media, a few calcium deposits were seen by day 7, and the amount of calcium deposits rapidly increased with time, especially at day 14 and 21. With 200 μM citrate

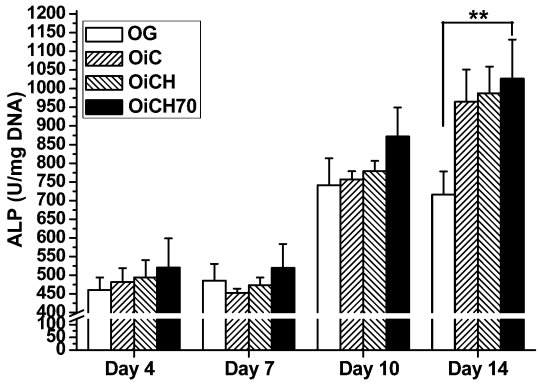

Fig. 8 ALP activity of osteogenic differentiated hMSC triggered by iCMBA/HA degradation products. $^{**}p < 0.01$.

supplementation in OG media, more calcium deposits were observed after day 7 compared to the pure OG group with differences becoming more obvious with prolonged time.

3.3.2 Effect of citrate on calcium deposit formation.

3.3.3 Citrate release from iCMBA/HA 70% (iCH70) composite. To mimic the citrate release process of iCMBA/HA in practical situation when being applied *in vivo*, iCH70 was chosen as the representative in citrate release studies. From Fig. 10, it can be seen that, after 2 days of release, the citrate concentration was already around 200 μM. The citrate concentrations increased to around 1000 μM with no significant increase during the later

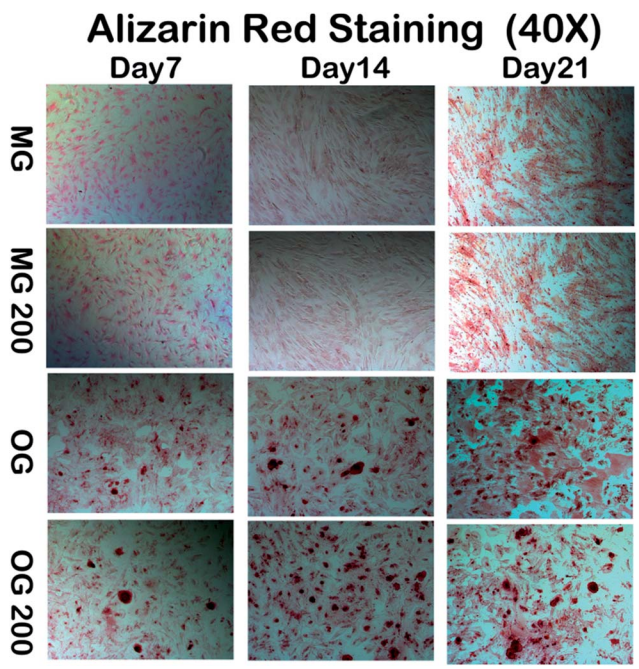

Fig. 9 Alizarin Red Staining for calcium deposit in hMSC cultures treated with growth media (MG), growth media with 200 μM citrate supplement (MG200), osteogenic media (OG), osteogenic media with 200 μM citrate supplement (OG200) at the 7th, 14th, and 21st day. Citrate in markedly enhanced calcium deposit formation of osteogenic differentiated hMSCs (Alizarin Red Staining, 40×).

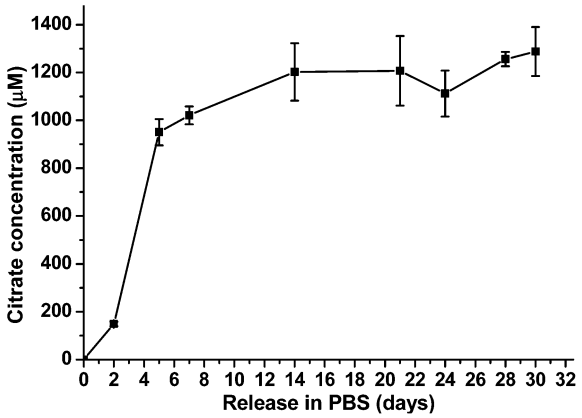

Fig. 10 Cumulative citrate release in PBS (pH 7.4) at 37 °C.

time intervals (to 30 days), indicating that it is possible to reach an effective concentration to promote calcium deposit formation when applied *in vivo*.

3.4 Biological performance of iCMBA/HA *in vivo*

Because of the abovementioned advantages, iCH70 was chosen as a representative material for *in vivo* evaluation using reproducible comminuted radial facture model on rabbits. Computer tomography (CT) analysis, three-point bending test, and histological examination were conducted 4, 8, and 12 weeks post-operation.

3.4.1 Micro CT. Micro-CT analysis data is shown in Fig. 11. Bone mineral content (BMC) and bone mineral density (BMD) values in the iCMBA/HA group (iCH70) at three pre-determined time points were 388 ± 12 mg and 122 ± 7 mg cm^{-3} (4 week), 417 ± 30 mg and 133 ± 6 mg cm^{-3} (8 week), 427 ± 23 mg and 143 ± 8 mg cm^{-3} (12 week), respectively, which were all higher than those of the blank control group. The results in Fig. 11 indicate that at all time points, enhanced bone formation can be detected in the iCMBA/HA group compared to blank control group, indicating the beneficial effects of iCMBA/HA composites to bone healing in the early stages after injury.

3.4.2 Biomechanical test for explants. Biomechanical testing, an important index of the quality of bone healing, was assessed by three-point bending test (Fig. 12). The maximal loads of radial bone in iCMBA/HA group after 4, 8, and 12 weeks were 130 ± 5, 150 ± 4 and 178 ± 7.8 N, respectively, which were significantly higher than that in blank control group (103 ± 6, 125 ± 5 and 146 ± 7 N, respectively) at every predetermined time interval ($P < 0.05$).

3.4.3 Histological staining. Undecalcified histological assessment was conducted to assess new bone formation and microstructure in the area of interest (Fig. 13). Masson's trichrome staining results revealed the following: (1) iCH70 bone substitute degraded almost completely in 4 weeks with HA particles left scattered at the implant site; (2) At 12 weeks, HA particles were almost completely incorporated into new bone in the iCH70 bone substitute group and radial bone structure was found to be more organized compared to that in blank control group. Decalcified histological assessment was conducted to assess vascular formation and cell immigration in the area of interest (Fig. 13). H&E staining results (Fig. 13) revealed that in iCH70 group, the vascular formation was slightly higher, but generally comparable to that in blank control group at the 4-week time interval.

These three results indicate the following: (1) an increase in new bone formation and mineralization (calcium deposits) was found in iCH70 group, especially in the first four weeks after injection; (2) higher quality healing of comminuted radial bone was observed in the iCH70 group with higher maximal strengths in the biomechanical test; (3) iCMBA/HA bone substitutes can promote bone mass formation and improve new-formed bone quality. The possible reasons for these findings could be found in the histological examination: (1) neovascularization was present deep into the bone substitutes with the help of proper degradation of the bone substitutes, offering better blood supply to bring more nutrition for cell immigration and survival (Fig. 12); (2) the host bone could efficiently take in HA particles left by degrading polymer for new bone formation, which could speed up bone regeneration (see Fig. 10); and (3) more organized bone microstructure, especially cortical bone, was achieved due to better bone piece alignment (Fig. 13).

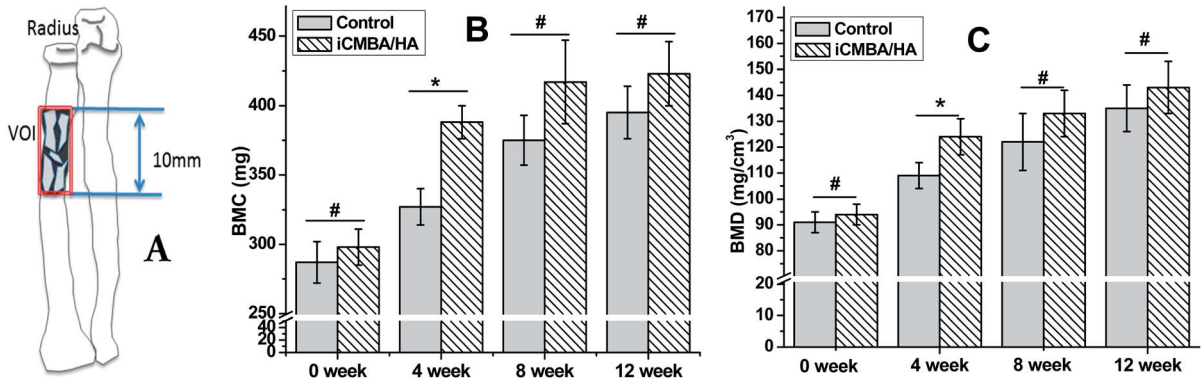

Fig. 11 Micro/CT analysis of comminuted fracture area of radius bone. Volume of interest (VOI) in analysis (A), bone mineral content (B) and bone mineral density (C). *: significant difference ($p < 0.05$), #: no significant difference ($p > 0.05$).

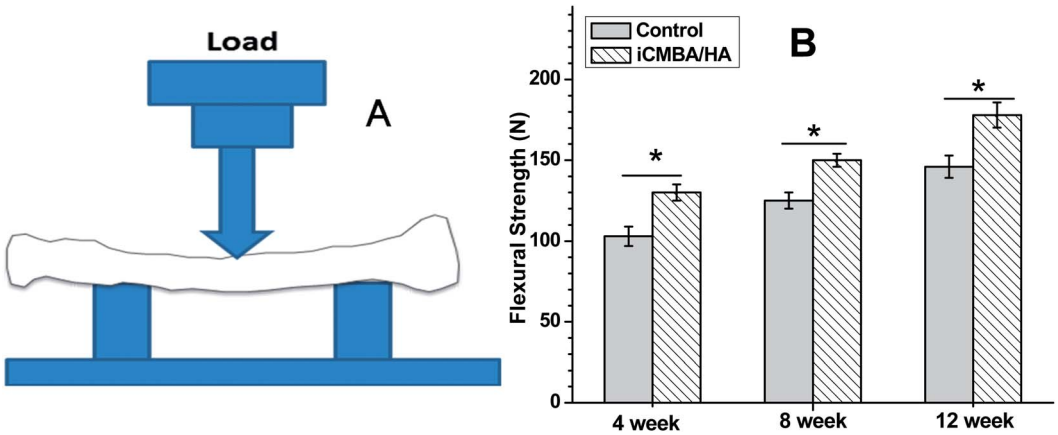

Fig. 12 Three-point-bending test was performed of on MTS machine for comminuted fracture area of radius bone. Maximal flexural strength was recorded. *: significant difference ($p < 0.05$).

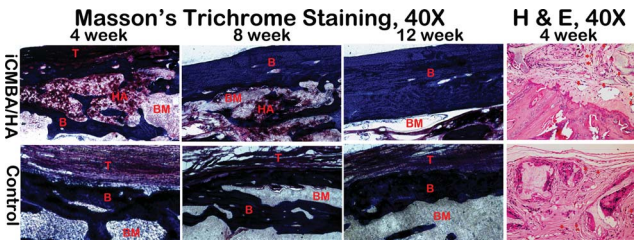

Fig. 13 Masson's trichrome staining (undecalcified hard tissue sections at week 4, 8 and 12) and hematoxylin and eosin (H&E) staining (decalcified section at week 4) of iCMBA/HA and control groups. After the fast degradation of iCMBA/HA composites, hydroxyapatite particles were scattered around and consequently incorporated into the new bone formation, thicker cortical bone with more organized microstructure were observed in iCMBA/HA group compared to control group (Masson's trichrome staining, 40×). Compared to control group, parallel new vessel formation was observed in iCMBA/HA group after 4 weeks of injection, which indicates that there was no inhibiting effect on neovasculation from iCMBA/HA (H&E staining, 40×). T: fibrous tissue; B: bone; HA: hydroxyapatite particle; BM: bone marrow cavity.

3.5 Citrate and HA contributions to calcium deposit formation

Mineralization is known to be a process controlled by multiple factors. Both citrate and HA in the iCMBA/HA bone substitute were supposed to play important roles in bone formation and mineralization and can explain the performance of iCMBA/HA for bone formation *in vivo*. For HA, we introduced it into bone material design to take advantage of its osteoconductivity, and based on the results of *in vitro* mineralization test of iCMBA/HA in SBF 5X, we confirmed its positive effect on mineralization (calcium deposit) on the surface of iCH70 (Fig. 5).

However, for citrate, except for its confirmed positive role in the expression of ALP, a protein marker of bone formation,[27] its role in mineralization has not been determined to date. We are the first to experimentally investigate citrate's effect in calcium deposit formation of hMSC. Based on our Alizarin Red staining results, we confirmed that citrate promotes calcium deposit formation during osteogenic differentiation of hMSC. In particular, for differentiated hMSC, exogenous citrate significantly promotes mineralization in the culture while it lost this function in undifferentiated hMSC. Therefore, we deem that citrate places positive effect on the mineralization of differentiated hMSC at the osteogenic stage.

4. Conclusions

We have confirmed that mussel-inspired citrate-based adhesive iCMBA/HA bone substitute may serve as an ideal candidate for CBF treatment as necessary supplement to instrumented fixation. On the one hand, it shows favorable injectability and setting time, as well as suitable physical properties (sol content, swelling and degradation) and mechanical properties (cohesion and adhesion strength) *in vitro*. iCMBA/HA also possesses minimal cytotoxicity, and due to the ester-bond backbone of iCMBA pre-polymer, this citrate-based adhesive iCMBA/HA bone substitute degrades at a rate favorable to neovascularization and bone growth to ultimately provide a positive effect on increasing bone mass and bone strength recovery. The strong adhesive strength is a great benefit to maintain proper bone piece alignment, which is considered as one important factor for bone formation. On the other hand, we are the first to experimentally find that citrate, which is the distinctive degradation product of iCMBA/HA composites, significantly promotes mineralization and bone formation of differentiated hMSC in osteogenic media. Therefore, adhesive iCMBA/HA bone composites could potentially serve as ideal bone grafts for the treatment of CBF.

Acknowledgements

This work was supported in part by the National Institutes of Health (NIH) Awards (NIBIB EB012575, NCI CA182670, NHLBI HL118498), and the National Science Foundation (NSF) Awards (DMR1313553, CMMI 1266116), and the National Natural Science Foundation of China (NSFC, grant 31228007).

Notes and references

1 E. Stöhr and U. Holz, *Orthopade*, 2000, **29**, 342.
2 R. Teasdall, F. H. Savoie and J. L. Hughes, *Clin. Orthop. Relat. Res.*, 1993, **292**, 37.
3 D. Taylor, J. G. Hazenberg and T. C. Lee, *Nat. Mater.*, 2007, **6**, 263.
4 A. Galperin, R. A. Oldinski, S. J. Florczyk, J. D. Bryers, M. Zhang and B. D. Ratner, *Adv. Healthcare Mater.*, 2013, **2**, 872.
5 H. Yuan, H. P. Fernandes Habibovic, J. de Boer, A. M. Barradas, A. de Ruiter, W. R. Walsh, C. A. van Blitterswijk and J. D. de Bruijn, *Proc. Natl. Acad. Sci. U. S. A.*, 2010, **107**, 13614.
6 B. B. Mandal BB, A. Grinberg, E. S. Gil, B. Panilaitis and D. L. Kaplan, *Proc. Natl. Acad. Sci. U. S. A.*, 2012, **109**, 7699.
7 N. Annabi, A. Tamayol, J. A. Uquillas, M. Akbari, L. E. Bertassoni, C. Cha, G. Camci-Unal, M. R. Dokmeci, N. A. Peppas and A. Khademhosseini, *Adv. Mater.*, 2014, **26**, 85.
8 S. K. L. Levengood and M. Zhang, *J. Mater. Chem. B*, 2014, **2**, 3161.
9 P. Ni, Q. Ding, M. Fan, J. Liao, Z. Qian, J. Luo, X. Li, F. Luo, Z. Yang and Y. Wei, *Biomaterials*, 2014, **35**, 236.
10 B. Chen, Y. Li, D. Xie, X. Yang and Z. Zheng, *Eur. Spine. J.*, 2011, **20**, 1272.
11 A. Sugawara, K. Asaoka and S.-J. Ding, *J. Mater. Chem. B*, 2013, **1**, 1081.
12 S. V. Dorozhkin, *Int. J. Mater. Chem.*, 2011, **1**, 1.
13 J. Guo, D. Y. Nguyen, R. T. Tran, Z. Xie, X. Bai and J. Yang, *Natural and Synthetic Biomedical Polymers*, 2014, p. 259.
14 M. G. Solari, E. Spangler, A. Lee and R. Wollstein, *Hand Surg.*, 2011, **16**, 223.
15 Y. Wu, L. Wang, B. Guo and P. X. Ma, *J. Mater. Chem. B*, 2013, **2**, 3674.
16 A. Cipitria, C. Lange, H. Schell, W. Wagermaier, J. C. Reichert, D. W. Hutmacher, P. Fratzl and G. N. Duda, *J. Bone Miner. Res.*, 2012, **27**, 1275.
17 M. D'Este and D. Eglin, *Acta Biomater.*, 2013, **9**, 5421.
18 Z. Xia, M. M. Villa and M. Wei, *J. Mater. Chem. B*, 2014, **2**, 1998.
19 J. D. Kretlow, S. Young, L. Klouda, M. Wong and A. G. Mikos, *Adv. Mater.*, 2009, **21**, 3368.
20 A. Pompili, F. Caroli, L. Carpanese, M. Caterino, L. Raus, G. Sestili and E. Occhipinti, *J. Neurosurg.*, 1998, **89**, 236.
21 K. H. Bae, L.-S. Wang and M. Kurisawa, *J. Mater. Chem. B*, 2013, **1**, 5371.
22 M. Mehdizadeh, H. Weng, D. Gyawali, L. Tang and J. Yang, *Biomaterials*, 2012, **33**, 7972.
23 Q. Lu, E. Danner, J. H. Waite, J. N. Israelachvili, H. Zeng and D. S. Hwang, *J. R. Soc., Interface*, 2013, **10**, 20120759.
24 C. Leimgruber, *Divulg. Cult. Odontol.*, 1965, **103**, 3.
25 R. L. Hartles, *Adv. Oral Biol.*, 1964, **1**, 225.
26 E. Davies, K. H. Müller, W. C. Wong, C. J. Pickard, D. G. Reid, J. N. Skepper and M. J. Duer, *Proc. Natl. Acad. Sci. U. S. A.*, 2014, **111**, E1354.
27 R. T. Tran, L. Wang, C. Zhang, M. Huang, W. Tang, C. Zhang, Z. Zhang, D. Jin, B. Banik, J. L. Brown, Z. Xie, X. Bai and J. Yang, *J. Biomed. Mater. Res., Part A*, 2014, **102**, 2521.
28 Y. Y. Hu, A. Rawal and K. Schmidt-Rohr, *Proc. Natl. Acad. Sci. U. S. A.*, 2010, **107**, 22425.
29 L. C. Costello and R. B. Franklin, *J. Regener. Med. Tissue Eng.*, 2013, **2**, 1.
30 L. C. Costello, R. B. Franklin, M. A. Reynolds and M. Chellaiah, *Open Bone J.*, 2012, **4**, DOI: 10.2174/1876525401204010027.
31 J. Yang, A. R. Webb and G. A. Ameer, *Adv. Mater.*, 2004, **16**, 511.
32 H. Qiu, J. Yang, P. Kodali, J. Koh and G. A. Ameer, *Biomaterials*, 2006, **27**, 5845.
33 M. Mehdizadeh and J. Yang, *Macromol. Biosci.*, 2013, **13**, 271.
34 D. Gyawali, P. Nair, P. H. Kim and J. Yang, *Biomater. Sci.*, 2013, **1**, 52.
35 J. Guo, Z. Xie, R. T. Tran, D. Xie, D. Jin, X. Bai and J. Yang, *Adv. Mater.*, 2014, **26**, 1906.
36 Y. Guo, R. T. Tran, D. Xie, Y. Wang, D. Y. Nguyen, E. Gerhard, J. Guo, J. Tang, Z. Zhang, X. Bai and J. Yang, *J. Biomed. Mater. Res., Part A*, 2014, DOI: 10.1002/jbm.a.35228.
37 A. Oyane, H.-M. Kim, T. Furuya, T. Kokubo, T. Miyazaki and T. Nakamura, *J. Biomed. Mater. Res., Part A*, 2003, **65**, 188.
38 I. Kallai, O. Mizrahi, W. Tawackoli, Z. Gazit, G. Pelled and D. Gazit, *Nat. Protoc.*, 2011, **6**, 105.
39 B. Chen, Y. Li, X. Yang and D. Xie, *J. Orthop. Sci.*, 2012, **17**, 70.
40 B. Chen, Y. Li, X. Yang and D. Xie, *Calcif. Tissue Int.*, 2013, **93**, 481.
41 O. Leppänen, H. Sievänen, J. Jokihaara, I. Pajamäki and T. L. N. Järvinen, *J. Bone Miner. Res.*, 2006, **21**, 1231.
42 B. Chen, D. Xie, Z. Zheng, W. Lu, C. Ning, Y. Li, F. Li and W. Liao, *Osteoporosis Int.*, 2011, **22**, 265.
43 M. I. Santos and R. L. Reis, *Macromol. Biosci.*, 2010, **10**, 12.
44 A. A. Kocher, M. D. Schuster, M. J. Szabolcs, S. Takuma, D. Burkhoff, J. Wang, S. Homma, N. M. Edwards and S. Itescu, *Nat. Med.*, 2001, **7**, 430.
45 H. Winet, J. Y. Bao and R. Moffat, *J. Bone Miner. Res.*, 1990, **5**, 19.
46 S. Browne and A. Pandit, *J. Mater. Chem. B*, 2014, **2**, 6692.
47 R. Smeets, K. Endres, G. Stockbrink, H. Hanken, B. Hermanns Sachweh, R. Marx, M. Heiland, M. Blessmann, K.-D. Wolff and A. Kolk, *J. Biomed. Mater. Res., Part A*, 2013, **101**, 2058.

